PHYSICAL REVIEW D **89,** 056002 (2014)

Possible generation of anomalously soft quark excitations at nonzero temperature: Nonhyperbolic dispersion of the parapion and van Hove singularity

Masakiyo Kitazawa,[1] Teiji Kunihiro,[2] and Yukio Nemoto[3]

[1]*Department of Physics, Osaka University, Toyonaka, Osaka 560-0043, Japan*
[2]*Department of Physics, Kyoto University, Kyoto 606-8502, Japan*
[3]*Department of Physiology, St. Marianna University School of Medicine, Kawasaki, Kanagawa 216-8511, Japan*

(Received 10 December 2013; published 6 March 2014)

We study the quark spectrum at finite temperature near and above the pseudocritical temperature of the chiral phase transition incorporating the effects of the collective modes with the quantum number of the sigma (parasigma) and pion (parapion) in a chiral effective model with a nonzero current quark mass. Below the pion zero-binding temperature where the pionic modes are bound, the quark self-energy has van Hove singularity induced by the scattering of quarks with the composite bound pions with a nonhyperbolic dispersion curve. This singularity is found to cause a drastic change in the quark spectrum from that in the mean field picture near the pseudocritical temperature: The quark spectrum has an unexpected sharp peak at an energy considerably lower than the constituent quark mass, while the spectrum approaches the mean field one at high temperatures. We clarify that the emergence of this anomalous structure of the quark spectral function originates from the composite nature of the pionic modes with a non-Lorentz invariant dispersion relation in the medium at finite temperature.

DOI: 10.1103/PhysRevD.89.056002 PACS numbers: 11.30.Rd, 21.65.Qr

I. INTRODUCTION

The exploration of the nature of the hot medium near the phase boundary of chiral and deconfinement phase transitions is an intriguing subject in quantum chromodynamics (QCD). Experimental results in heavy-ion collisions at the Relativistic Heavy Ion Collider (RHIC) [1] and the Large Hadron Collider (LHC) [2] suggest that the quark-gluon medium near the phase boundary is a strongly interacting system. The properties of the hot medium are also actively investigated by the lattice QCD Monte Carlo simulations, which have recently revealed that the phase transition between hadronic and quark-gluon media at vanishing baryon chemical potential is a smooth crossover without a sharp boundary [3]. The lattice simulations also suggest that the thermodynamic observables including higher-order fluctuations of conserved charges are well described by the hadron resonance gas model below the pseudocritical temperature $T_{\rm PC}$, but such a picture breaks down in a narrow range of temperature (T) near $T_{\rm PC}$ [3,4]. This result indicates that, despite the crossover nature, the hot medium suddenly changes its character from that of a simple system composed of approximately free hadrons to a highly correlated system with unknown but intriguing degrees of freedom in the vicinity of $T_{\rm PC}$.

To explore the nature of the hot medium above $T_{\rm PC}$, it is natural to begin with an investigation of the existence and properties of collective excitations having the quantum numbers of the quarks and gluons. As for collective modes carrying a quark quantum number, it is notable that recent nonperturbative analyses on the quark spectral function on the lattice [5–7] and Schwinger-Dyson approaches [8–12] indicate the existence of such quasiparticle excitations even for temperatures not much greater than $T_{\rm PC}$.

For temperatures near but above $T_{\rm PC}$, interesting ingredients come into play owing to the strong coupling. One of them is a possible existence of hadronic excitations that may survive the phase transition. Indeed, lattice simulations show that charm quarkonia can still exist as relatively stable states with an increasing width even well above $T_{\rm PC}$ [13]. Another example of such hadronic states is the soft modes of chiral phase transition [14]. When the chiral transition is not so strong first order, some specific collective modes of quarks and antiquarks have a chance to develop in the scalar (σ) and pseudoscalar (π) channels near the critical temperature in accordance with the enhancement of the fluctuations of the order parameter. Moreover the masses (peak position of the spectral function) of these collective modes decrease as the system approaches the critical point, and these modes are called the soft modes of chiral transition [14]: They become exactly massless at the critical temperature in the chiral limit.

When such soft modes exist above $T_{\rm PC}$, they can in turn affect the properties of the quasiquark excitations. This possibility was explored in Ref. [15] in a two-flavor Nambu–Jona-Lasinio (NJL) model as in Ref. [14] in the chiral limit. In this case, the chiral transition at nonzero T is of second order and the quark has no constituent quark mass above the critical temperature T_c, where the well-developed soft modes appear near T_c. It was shown that the

fermion spectrum at low momentum has a three-peak structure for $T \sim T_c$; the fermion spectrum acquires a sharp peak at low energy in addition to normal and plasmino modes having thermal masses.

It is worth mentioning that the emergence of the three-peak structure in the fermion spectrum is a universal phenomenon for fermion-boson systems at nonzero temperature T when the fermion mass m_f is not so large [16,17]; see also [18]. In Ref. [16], the fermion spectrum at nonzero T was investigated in a simple Yukawa model composed of a massless fermion and an *elementary* boson with mass m_b at the one-loop order, where the boson dispersion relation, $\omega_b = \omega_b(q)$, is simply assumed to be of the hyperbolic form $\omega_b(q) = \sqrt{m_b^2 + q^2}$ and the possible modification of it owing to the coupling to the fermion at $T \neq 0$ is neglected. It was found that the fermion spectrum at low momentum has a three-peak structure for $T \simeq m_b$. The existence of the sharp peak in the quark spectrum at low energy is later confirmed in various models and analyses incorporating higher-order contributions [8,11,19], in some of which the needed nonzero boson mass m_b is supplied by the thermal mass. On the other hand, it was shown in a Yukawa model with a massive fermion and an elementary massive boson [17] that the nonzero fermion mass m_f tends to suppress the appearance of the sharp peak at small energy that would be seen for $T \simeq m_b$: Such a peak can exist in the fermion spectrum only when the masses satisfy the condition $m_f \lesssim 0.2 m_b$.

The purpose of the present study is to extend the analysis in Ref. [15] to the case off the chiral limit with nonzero current quark mass m_0. With the explicit chiral symmetry breaking, the constituent quark mass takes nonzero values for all T, while the soft modes in the σ and π channels do not become massless. In view of the analysis in Ref. [17] on the effect of nonzero fermion mass and the fact that the nonzero mass of the bosonic modes would also act to suppress the thermal effect on the fermion spectrum, one might suspect that the interesting structure in the quark spectrum obtained in the chiral limit will be blurred by nonzero m_0. In this paper, we shall show that it is not the case. One of the basic facts is the existence of the composite pionic mode with a *stability* above $T_{\rm PC}$: Because the constituent quark mass takes a nonzero value above $T_{\rm PC}$, the soft pionic modes can be stable against the decay into a quark and an antiquark even above $T_{\rm PC}$ up to some temperature at least one-loop level [20]. We call the soft mode in the pionic channel existing above $T_{\rm PC}$ the para-pion. The other important ingredient leading to the results contrary to the naive suspect is a well-known fact that the dispersion relation $\omega_\pi(q)$ of the pionic mode in the medium at $T \neq 0$ is generically different from the hyperbolic form given by $\omega_{\rm rel}(q) = \sqrt{q^2 + [\omega_\pi(0)]^2}$ because of the violation of Lorentz symmetry at nonzero temperature and/or density [21,22]. We shall show that van Hove singularity [21,23–25] is brought about in the quark self-energy through the scattering of quarks with the pionic modes having such a modified dispersion relation, and the singularity drastically changes the quark spectrum. In particular, we find that the quark spectral function has a sharp peak at an energy significantly lower than the constituent quark mass, which is quite reminiscent of but has a different origin from that of the peak found in Refs. [8,11,15,16,19]. It will also be addressed that the modification of the quark spectrum with this mechanism is expected to take place when a bosonic mode that couples to the quark has a nonhyperbolic dispersion relation irrespective of the detailed structure of the dispersion relation. Indeed, possible phenomenological consequences of such a modified dispersion relation of the pionic mode in the hot and/or dense medium were discussed in various contexts by many authors [21,22,24].

The paper is organized as follows. The next section deals with the chiral soft modes. In Sec. III, we calculate the quark self-energy due to the soft modes and evaluate the quark spectral function. The numerical results are shown in Sec. IV. The final section is devoted to a summary and concluding remarks.

II. FLUCTUATION MODES

To study the fluctuation modes in the scalar (σ) and pseudoscalar (π) channels on the spectral properties of quarks near the phase boundary, we employ the two-flavor NJL model [26] as an effective model of low-energy QCD [20]

$$\mathcal{L} = \bar{\psi}(i\partial\!\!\!/ - m_0)\psi + G_S[(\bar{\psi}\psi)^2 + (\bar{\psi} i\gamma_5 \boldsymbol{\tau}\psi)^2], \quad (1)$$

with $\boldsymbol{\tau}$ being the flavor SU(2) Pauli matrices and the nonzero current quark mass $m_0 = 5.5$ MeV. The coupling constant $G_S = 5.5$ GeV^{-2} and the three-dimensional cutoff $\Lambda = 631$ MeV are determined so as to reproduce the pion mass, the pion decay constant, and the quark condensate in vacuum [20]. We can expect that there will be no essential systematic uncertainty in the numerical results to be presented in the present work, once the parameters are fitted to reproduce the physical values in vacuum, although another parameter set may be possible for that.

The constituent quark mass in the self-consistent mean-field approximation (MFA) at $T \neq 0$ is given by

$$m = m_0 - 2G_S\langle\bar{\psi}\psi\rangle, \quad (2)$$

with the chiral condensate $\langle\bar{\psi}\psi\rangle$ evaluated with the mass m. In Fig. 1, we show the T dependence of the resultant m. The figure shows that in the vacuum $m = 337$ MeV is significantly larger than m_0 as a consequence of the spontaneous chiral symmetry breaking. For nonzero T, the constituent quark mass smoothly decreases in accordance with the chiral restoration in medium. Because of the crossover

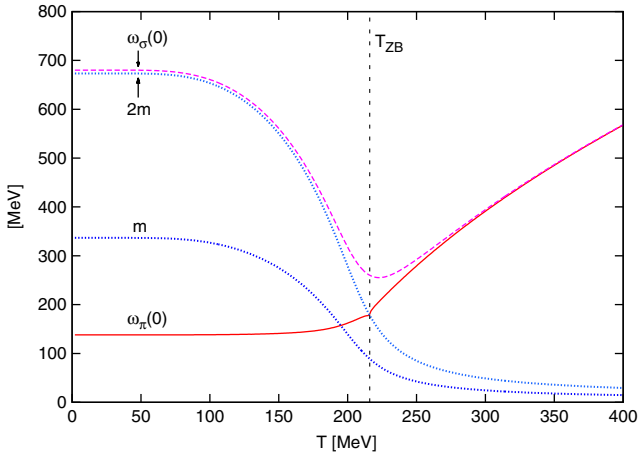

FIG. 1 (color online). Temperature dependence of the constituent quark mass m, and the solution of Eq. (7) at zero momentum for π and σ channels, $\omega_\pi(0)$ and $\omega_\sigma(0)$, respectively. Twice the constituent quark mass is also plotted. The vertical line shows the pion zero-binding temperature $T_{\rm ZB}$.

nature, there are several definitions of the pseudocritical temperature $T_{\rm PC}$. One can, for example, define $T_{\rm PC}$ as the temperature at which the magnitude of the chiral condensate becomes half the vacuum value. With this definition we have $T_{\rm PC} \simeq 192$ MeV. Another possible choice is to use the dynamic chiral susceptibility in the spacelike region [27], which diverges at the critical point when the transition is second order [28]: When $T_{\rm PC}$ is defined as the temperature where the dynamic chiral susceptibility with the momentum $|\boldsymbol{q}| = 10$ MeV has the maximum, we have $T_{\rm PC} \simeq 206$ MeV. One can also define $T_{\rm PC}$ as the temperature at which the static chiral susceptibility has the maximum, which gives $T_{\rm PC} \simeq 211$ MeV in this model.

The properties of the fluctuation modes in the σ and π channels are encoded in the retarded propagator of these channels, $D^R_\sigma(\boldsymbol{q}, q_0)$ and $D^R_\pi(\boldsymbol{q}, q_0)$, respectively. In the random phase approximation, these propagators are given by

$$D^R_{\sigma(\pi)}(\boldsymbol{q}, q_0) = -\frac{2G_S}{1 + 2G_S Q^R_{\sigma(\pi)}(\boldsymbol{q}, q_0)}, \tag{3}$$

with the one-loop quark-antiquark polarization functions $Q^R_{\sigma(\pi)}(\boldsymbol{q}, q_0)$. The diagrammatic representation of Eq. (3) is shown in the upper part of Fig. 2. The imaginary-time (Matsubara) propagators corresponding to $Q^R_{\sigma(\pi)}(\boldsymbol{q}, q_0)$ are

$$\mathcal{Q}_\sigma(\boldsymbol{q}, \nu_n) = T\sum_m \int \frac{d^3p}{(2\pi)^3} \mathrm{Tr}[\mathcal{G}_0(\boldsymbol{p}, \omega_m)\mathcal{G}_0(\boldsymbol{q}+\boldsymbol{p}, \nu_n + \omega_m)], \tag{4}$$

$$\mathcal{Q}_\pi(\boldsymbol{q}, \nu_n) = \frac{T}{3}\sum_m \int \frac{d^3p}{(2\pi)^3} \mathrm{Tr}[i\gamma_5 \boldsymbol{\tau} \mathcal{G}_0(\boldsymbol{p}, \omega_m) \times i\gamma_5 \boldsymbol{\tau} \mathcal{G}_0(\boldsymbol{q}+\boldsymbol{p}, \nu_n + \omega_m)], \tag{5}$$

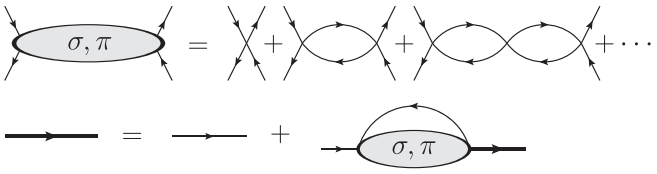

FIG. 2. Diagrammatic representation of the propagators of the bosonic and fermionic modes in this study. The shaded area of the upper diagram represents the propagator of the sigma or pionic modes, $D^R_{\sigma(\pi)}(\boldsymbol{q}, \omega_n)$ in Eq. (3), while the lower line represents the quark propagator defined in Eq. (14).

where $\mathcal{G}_0(\boldsymbol{p}, \omega_n) = [i\omega_n\gamma_0 - \boldsymbol{p}\cdot\boldsymbol{\gamma} - m]^{-1}$ is the quark propagator in the MFA, and $\nu_n = 2n\pi T$ and $\omega_n = (2n+1)\pi T$ denote the Matsubara frequencies for bosons and fermions, respectively, and Tr denotes the trace over the color, flavor, and Dirac indices.

After the summation of the Matsubara frequency and the analytic continuation with a replacement $i\nu_n \to q_0 + i\eta$ in Eqs. (4) and (5), we obtain the corresponding retarded polarization functions $Q^R_\sigma(\boldsymbol{q}, q_0)$ and $Q^R_\pi(\boldsymbol{q}, q_0)$. For the numerical calculation of $Q^R_{\sigma(\pi)}(\boldsymbol{q}, q_0)$, we first calculate their imaginary parts and then evaluate the real parts with the Kramers-Kronig relation

$$\mathrm{Re}Q^R_{\sigma(\pi)}(\boldsymbol{q}, q_0) = -\frac{1}{\pi}\mathrm{P}\int_{-\Lambda'}^{\Lambda'} dq_0{}' \frac{\mathrm{Im}Q^R_{\sigma(\pi)}(\boldsymbol{q}, q_0{}')}{q_0 - q_0{}'}, \tag{6}$$

where P denotes the principal value. The cutoff of the $q_0{}'$ integral in Eq. (6), $\Lambda' = 2\sqrt{\Lambda^2 + m^2}$, must be chosen to be the same as that used in the evaluation of the static quantities [20], which ensures that $D^R_\sigma(\boldsymbol{q}, q_0)$ at small $\boldsymbol{q}$ and q_0 diverges at the critical point of second order phase transition determined in the MFA [15].

The imaginary parts of $Q^R_\sigma(\boldsymbol{q}, q_0)$ and $Q^R_\pi(\boldsymbol{q}, q_0)$ are proportional to the difference between the decay and creation rates of each mode. It is easily shown that $\mathrm{Im}Q^R_{\sigma(\pi)}(\boldsymbol{q}, q_0)$ take nonzero values for $|q_0| > \sqrt{q^2 + 4m^2}$ and $|q_0| < q$, with $q = |\boldsymbol{q}|$. The decay process for $q_0 > \sqrt{q^2 + 4m^2}$ in each channel corresponds to that into a quark and an antiquark, while the one in the spacelike region represents the Landau damping.

Collective modes in the π channel are characterized by the poles of the propagator $D^R_\pi(\boldsymbol{q}, q_0)$. When a pole is on the real axis, its location, $q_0 = \omega_\pi(q)$, i.e., the dispersion relation of the bound pionic modes, is determined by solving

$$\mathrm{Re}[D^R_\pi(\boldsymbol{q}, \omega_\pi(q))]^{-1} = -\frac{1}{2G_S} - \mathrm{Re}Q^R_\pi(\boldsymbol{q}, \omega_\pi(q)) = 0, \tag{7}$$

with the residue $Z_\pi(q)$ of the pole

$$\frac{1}{Z_\pi(q)} = -\frac{1}{\pi}\frac{\partial[D_\pi^R(\boldsymbol{q},\omega_\pi(q))]^{-1}}{\partial q_0}\bigg|_{q_0=\omega_\pi(q)} = -\frac{1}{\pi}\frac{\partial Q_\pi^R(\boldsymbol{q},\omega_\pi(q))}{\partial q_0}\bigg|_{q_0=\omega_\pi(q)}. \quad (8)$$

The pole on the real axis can exist in the range $q < |\omega_\pi(q)| < \sqrt{q^2+4m^2}$ in which $\mathrm{Im}Q_\pi^R(\boldsymbol{q},q_0)$ vanishes. While a solution of Eq. (7) no longer corresponds to a bound pole when $\omega_\pi(q)$ is outside this range, it is known that $\omega_\pi(q)$ approximately represents the real part of the corresponding pole on the lower-half complex-energy plane.

In the vacuum, $D_\pi^R(\boldsymbol{q},q_0)$ has a bound pole on the real axis as the pseudo-Nambu-Goldstone pion. As T is raised, the pionic modes eventually become unstable against the decay into a quark and an antiquark, as the constituent quark mass m becomes smaller while the rest mass of pions, $\omega_\pi(0)$, becomes larger as shown in Fig. 1 [20]. We denote the temperature at which the rest pionic modes become unstable by T_{ZB} and call it the pion zero-binding temperature. Since the rest pionic modes are unstable for $\omega_\pi(0) > 2m$, T_{ZB} is determined by

$$[D_\pi^R(\boldsymbol{0},2m)]^{-1}_{T=T_{\mathrm{ZB}}} = 0. \quad (9)$$

In our model, the dissociation takes place at $T_{\mathrm{ZB}} = 216$ MeV, which is depicted in Fig. 1 by the vertical line. Note that the value of T_{ZB} is higher than T_{PC} irrespective of the choices of the definition discussed before. In Fig. 1, the solution of Eq. (7) for the σ channel with $q = 0$, $\omega_\sigma(0)$, is also shown. As in the figure, the solution is always in the continuum, i.e., $\omega_\sigma(0) > 2m$, which means that the stable σ mode does not exist in our model [20].

In the vacuum, the dispersion relation of the pions should obey the relativistic one

$$\omega_{\mathrm{rel}}(q) = \sqrt{q^2+[\omega_\pi(0)]^2}, \quad (10)$$

because of the Lorentz symmetry. In the medium at nonzero temperature and/or baryonic density, however, $\omega_\pi(q)$ can deviate from this form since the medium effect violates the Lorentz symmetry [21,22]. In Fig. 3 we show the dispersion relation of the bound pionic modes $\omega_\pi(q)$ at $T = 206$ MeV, which is slightly below T_{ZB}. One finds that $\omega_\pi(q)$ clearly deviates from the Lorentz-invariant form shown by the dashed line in the figure. It is also notable that $\omega_\pi(q)$ enters the continuum and the pionic modes become unstable at $q \simeq 360$ MeV. This result indicates that a pionic mode moving with a large velocity relative to the medium can become unstable even when the rest pion can exist as a bound state. As we will see later, the deviation of $\omega_\pi(q)$ from the relativistic form plays a crucial role for the emergence of the unexpected behaviors of the quark spectrum for $T \lesssim T_{\mathrm{ZB}}$.

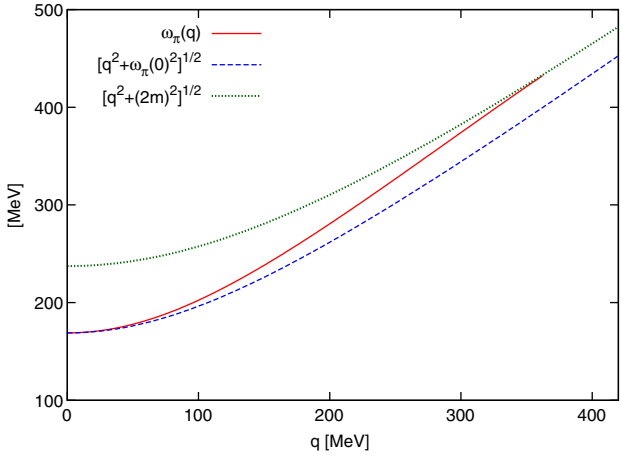

FIG. 3 (color online). The dispersion relations of the pionic modes (solid line) and the relativistic dispersion relation for free particles $\sqrt{q^2+[\omega_\pi(0)]^2}$ (dashed line) at $T = 206$ MeV. The dotted line denotes the continuum threshold $\sqrt{q^2+4m^2}$.

The result in Fig. 3 shows that the pion dispersion relation near T_{ZB} is steeper than the relativistic one, Eq. (10). We note that this result in our model is to some extent affected by the explicit breaking of Lorentz symmetry due to the three-dimensional cutoff besides the genuine medium effect. In fact, the dispersion relation $\omega_\pi(q)$ in our model slightly deviates from Eq. (10) toward a steeper direction even in the vacuum. Nonetheless, as shown in Ref. [20], there are some advantages to adopt this cutoff, and we can show that the resultant van Hove singularity near the pseudocritical point appears irrespective of the cutoff scheme as mentioned in Sec. IV B.

The qualitative structure of the pion dispersion relation in the medium has been discussed in various contexts [21,22]. Among them, it is shown in Ref. [22] that the pion dispersion relation at sufficiently low temperature becomes shallower than in the vacuum on the basis of the chiral symmetry and Nambu-Goldstone nature of the pions. On the other hand, it seems that there is no conclusive argument on the behavior of the dispersion relation at T above the pseudocritical temperature. Because the structure of the pion dispersion relation plays a crucial role on the quark spectrum, we will come back to this point later in Sec. IV.

Before closing this section, we introduce the spectral function of the sigma (pionic) mode

$$\rho_{\sigma(\pi)}(\boldsymbol{q},q_0) = -\frac{1}{\pi}\mathrm{Im}D^R_{\sigma(\pi)}(\boldsymbol{q},q_0). \quad (11)$$

When $D_\pi^R(\boldsymbol{q},q_0)$ has a bound pole, $\rho_\pi(\boldsymbol{q},q_0)$ is decomposed as

$$\rho_\pi(\boldsymbol{q},q_0) = \rho_\pi^{\mathrm{cont}}(\boldsymbol{q},q_0) + \rho_\pi^{\mathrm{pole}}(\boldsymbol{q},q_0), \quad (12)$$

where $\rho_\pi^{\mathrm{cont}}(\boldsymbol{q},q_0)$ is the continuum part taking nonzero values for $|q_0| > \sqrt{q^2+4m^2}$ and $|q_0| < q$, and

$$\rho_\pi^{\rm pole}(\boldsymbol{q},q_0)=Z_\pi(q)[\delta(q_0-\omega_\pi(q))-\delta(q_0+\omega_\pi(q))]. \quad (13)$$

III. QUARK SPECTRAL FUNCTION

The collective modes composed of quarks and antiquarks have a natural coupling with quarks, which in turn leads to a modification of the spectral properties of quarks, in particular, near the pseudocritical temperature. To show how this modification is significant, let us calculate the quark propagator coupled with the sigma and pionic modes in the random phase approximation [15]. The quark self-energy in the imaginary time formalism in this approximation is given by

$$\begin{aligned}\tilde{\Sigma}(\boldsymbol{p}=0,\omega_n)&\equiv\tilde{\Sigma}(\omega_n)\\&=-T\sum_m\int\frac{d^3q}{(2\pi)^3}\{\mathcal{D}_\sigma(\boldsymbol{q},\omega_n-\omega_m)\mathcal{G}_0(\boldsymbol{q},\omega_m)\\&\quad+3\mathcal{D}_\pi(\boldsymbol{q},\omega_n-\omega_m)i\gamma_5\mathcal{G}_0(\boldsymbol{q},\omega_m)i\gamma_5\}, \quad (14)\end{aligned}$$

with the Matsubara propagators of the sigma and pionic modes $\mathcal{D}_{\sigma(\pi)}(\boldsymbol{q},\nu_n)$. The quark propagator in this approximation is diagrammatically represented in Fig. 2. The factor 3 in the second term in Eq. (14) comes from the isospin degeneracy of pions. Since we are interested in excitation modes at low energy and low momentum, we limit our attention to the quark spectrum at zero momentum. The summation of the Matsubara frequency can be carried out analytically with an equivalent contour integral on the complex energy plane [29]. Then, after the analytic continuation $i\omega_n\to p_0+i\eta$, we obtain the retarded quark self-energy,

$$\Sigma^R(p_0)=\Sigma_\sigma^R(p_0)+\Sigma_\pi^R(p_0), \quad (15)$$

$$\begin{aligned}\Sigma_\sigma^R(p_0)&=\frac{1}{2}\sum_{s=\pm}\int\frac{d^3qd\omega}{(2\pi)^4}\frac{\pi\rho_\sigma(\boldsymbol{q},\omega)}{\omega-p_0+sE_q-i\eta}\\&\quad\times\left(\gamma^0+s\frac{m}{E_q}\right)\left[\coth\left(\frac{\omega}{2T}\right)+\tanh\frac{sE_q}{2T}\right], \quad (16)\end{aligned}$$

$$\begin{aligned}\Sigma_\pi^R(p_0)&=\frac{1}{2}\sum_{s=\pm}\int\frac{d^3qd\omega}{(2\pi)^4}\frac{3\pi\rho_\pi(\boldsymbol{q},\omega)}{\omega-p_0+sE_q-i\eta}\\&\quad\times\left(\gamma^0-s\frac{m}{E_q}\right)\left[\coth\left(\frac{\omega}{2T}\right)+\tanh\frac{sE_q}{2T}\right], \quad (17)\end{aligned}$$

with $E_q=\sqrt{\boldsymbol{q}^2+m^2}$. To avoid the ultraviolet divergence in Eqs. (16) and (17), we first determine the imaginary part that is free from the divergence, and then evaluate the real part with the Kramers-Kronig relation

$$\mathrm{Re}\Sigma_{\sigma(\pi)}^R(p_0)=-\frac{1}{\pi}\mathrm{P}\int_{-\Lambda}^{\Lambda}dp_0{}'\frac{\mathrm{Im}\Sigma_{\sigma(\pi)}^R(p_0{}')}{p_0-p_0{}'}, \quad (18)$$

where the energy integral is regularized by the cutoff Λ [15].

The retarded quark propagator for zero momentum,

$$G^R(p_0)=\frac{1}{(p_0+i\eta)\gamma^0-m-\Sigma^R(p_0)}, \quad (19)$$

is decomposed in terms of the projection operators $\Lambda_\pm=(1\pm\gamma_0)/2$ as

$$G^R(p_0)=G_+(p_0)\Lambda_+\gamma^0+G_-(p_0)\Lambda_-\gamma^0, \quad (20)$$

with

$$G_\pm(p_0)=\frac{1}{2}\mathrm{Tr}[G^R\gamma^0\Lambda_\pm]=\frac{1}{p_0+i\eta\mp m-\Sigma^\pm(p_0)}, \quad (21)$$

and $\Sigma^\pm(p_0)=(1/2)\mathrm{Tr}[\Sigma^R(p_0)\Lambda_\pm\gamma^0]$ [17]. The quasiquark and quasi-antiquark spectral functions are defined in accordance with Eq. (20) as

$$\rho_\pm(p_0)=-\frac{1}{\pi}\mathrm{Im}G_\pm(p_0). \quad (22)$$

For vanishing quark chemical potential, the charge conjugation symmetry of the medium ensures the symmetry relation $\rho_-(p_0)=\rho_+(-p_0)$. In the analysis of the quark spectrum in the next section, we thus concentrate on $\rho_+(p_0)$.

When the pionic modes have a bound pole, $\Sigma^\pm(p_0)$ are decomposed as

$$\Sigma^\pm(p_0)=\Sigma_\sigma^\pm(p_0)+\Sigma_{\pi\text{-pole}}^\pm(p_0)+\Sigma_{\pi\text{-cont}}^\pm(p_0), \quad (23)$$

where $\Sigma_\sigma^\pm(p_0)$ represents the contribution of Eq. (16). The contribution of the pionic modes, Eq. (17), is decomposed into those of $\rho_\pi^{\rm cont}(\boldsymbol{q},p_0)$ and $\rho_\pi^{\rm pole}(\boldsymbol{q},p_0)$ in Eq. (12). Using Eq. (13), one obtains

$$\begin{aligned}\mathrm{Im}\Sigma_{\pi\text{-pole}}^\pm(p_0)&=\frac{3}{4\pi^2}\sum_{r,s=\pm}\sum_{q=q_{sr}}\left[Z_\pi(\omega(q))\left(1\mp r\frac{m}{E_q}\right)\right.\\&\quad\left.\times q^2\left|\frac{d\mathcal{E}_s(q)}{dq}\right|^{-1}[1+n(r\omega(q))-f(sE_q)]\right], \quad (24)\end{aligned}$$

where q_{sr} with $r,s=\pm$ are solutions of

$$p_0=r\mathcal{E}_s(q_{sr})=r(sE_q+\omega_\pi(q))_{q=q_{sr}}, \quad (25)$$

with $\mathcal{E}_\pm(q)=\pm E_q+\omega_\pi(q)$, and the sum in Eq. (24) is taken for all the solutions of Eq. (25) for each s and r. The functions $n(x)$ and $f(x)$ are the Bose-Einstein and the Fermi-Dirac distribution functions, $n(x)=[\exp(x/T)-1]^{-1}$ and $f(x)=[\exp(x/T)+1]^{-1}$, respectively. The product of the first two factors in the second

line in Eq. (24) is proportional to the difference between the quark and pion-mode density of states, which is called the joint density of states. We note that $d\mathcal{E}_-(q)/dq = -dE_q/dq + d\omega_\pi(q)/dq$ has the meaning of the relative group velocity of the quark and the pion mode [21,22].

When $\omega_\pi(q)$ is of the relativistic (hyperbolic) form as given by Eq. (10), $\mathcal{E}_\pm(q)$ are monotonic functions of q. Equation (25) thus can have at most one solution for a given p_0. In the hot and dense medium, however, the deviation of $\omega_\pi(q)$ from the hyperbolic form can provide multiple solutions of these equations for a given p_0. The nonhyperbolic form of $\omega_\pi(q)$ can also lead to zeros of the relative group velocity $d\mathcal{E}_-(q)/dq$. For energies p_0 where $d\mathcal{E}_s(q_{sr})/dq$ vanish, $\mathrm{Im}\Sigma^\pm_{\pi\text{-pole}}(p_0)$ diverges owing to the divergence of the joint density of states $q^2[d\mathcal{E}_-(q)/dq]^{-1}$ with $q \neq 0$. Such singularities are known as the van Hove singularity [23,25,30]. As we will see in the next section, the van Hove singularities in $\mathrm{Im}\Sigma^\pm_{\pi\text{-pole}}(p_0)$, which manifest themselves as a consequence of the composite nature of bound pionic modes and medium effects, plays a crucial role to modify the quark spectral function significantly for $T \lesssim T_{\mathrm{ZB}}$.

IV. NUMERICAL RESULTS

A. Near pseudocritical temperature

Now we present the numerical results for the quark spectrum. In this subsection, we first investigate the effects of the bound pionic modes below T_{ZB} on the quark spectrum. To see this effect, we fix the temperature to $T = 206$ MeV throughout this subsection; this value is chosen as a typical temperature below T_{ZB} but not less than T_{PC}. As discussed in Sec. II, the dynamic chiral susceptibility has the largest peak in the spacelike region at this temperature [27]. As we will see in this subsection, however, the effect of the sigma mode does not have a significant contribution to the quark spectrum even for this temperature.

We first show $\rho_+(p_0)$ at $T = 206$ MeV in the upper panel of Fig. 4. The figure shows that the quark spectrum is significantly modified from the one in the MFA, $\rho_+(p_0) = \delta(p_0 - m)$, with $m \simeq 120$ MeV being the constituent quark mass in the MFA at this temperature. The quasiquark spectrum has a sharp peak at $p_0 \simeq 25$ MeV, which is considerably smaller than m. The spectral weight of this peak may be defined by

$$Z = \int_\Delta dp_0 \rho_+(p_0), \tag{26}$$

where Δ is a range of p_0 that well covers the peak structure. The numerical calculation gives $Z \simeq 0.16$, which is small but not negligible. The spectrum $\rho_+(p_0)$ also has a broad peak structure around $p_0 \simeq 160$ MeV. While there exists another peak at $p_0 \simeq -50$ MeV, the spectral weight of this peak is negligibly small.

To understand the origin of these structures in $\rho_+(p_0)$, the real and imaginary parts of $\Sigma^+(p_0)$ are shown in the middle and lower panels of Fig. 4, respectively. The real part of $\Sigma^+(p_0)$ determines the quasipoles of the quark, where the real part of the inverse propagator vanishes as

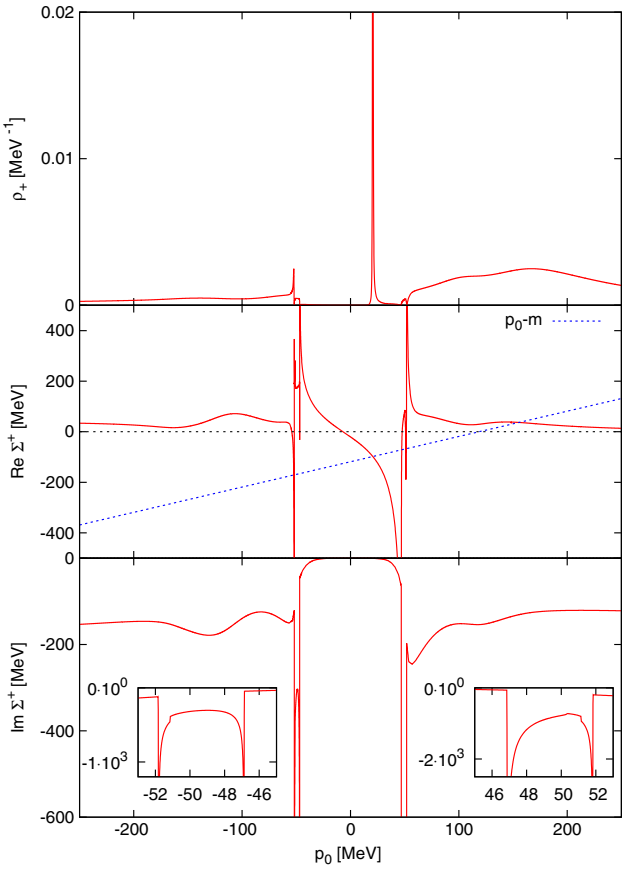

FIG. 4 (color online). The upper panel shows the quark spectral function $\rho_+(p_0)$ for $T = 206$ MeV. The middle and lower panels represent the real and imaginary parts of the corresponding quark self-energy $\Sigma^+(p_0)$. The dashed line in the middle panel denotes $p_0 - m$.

$$\mathrm{Re}[G_+(p_0)]^{-1} = p_0 - m - \mathrm{Re}\Sigma^+(p_0) = 0. \tag{27}$$

The quasipole gives approximate position of a peak in $\rho_+(p_0)$ when $\mathrm{Im}\Sigma^+(p_0)$ is small there [15]. The solutions of Eq. (27) are graphically determined by crossing points of $\mathrm{Re}\Sigma^+(p_0)$ and a line $p_0 - m$, which is drawn by the dashed line in the middle panel in Fig. 4. One finds that there exists a quasipole at $p_0 \simeq 25$ MeV corresponding to the sharp peak in $\rho_+(p_0)$. There also exists a quasipole around $p_0 \simeq 150$ MeV, but a clear peak corresponding to this quasipole does not appear in $\rho_+(p_0)$ because of the large $\mathrm{Im}\Sigma^+(p_0)$ around this energy. Although there are some more solutions of Eq. (27) around $p_0 = \pm 50$ MeV owing to the singular behaviors of $\mathrm{Re}\Sigma^+(p_0)$, clear peaks corresponding to these quasipoles are not formed in $\rho_+(p_0)$.

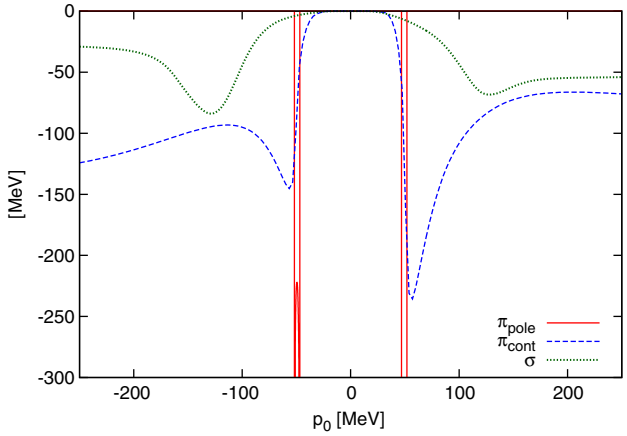

FIG. 5 (color online). Decomposition of $\mathrm{Im}\Sigma^{+}(p_0)$ into three parts, $\mathrm{Im}\Sigma^{+}_{\sigma}(p_0)$ (solid line), $\mathrm{Im}\Sigma^{+}_{\pi\text{-pole}}(p_0)$ (dotted line), and $\mathrm{Im}\Sigma^{+}_{\pi\text{-cont}}(p_0)$ (dashed line) at $T = 206$ MeV.

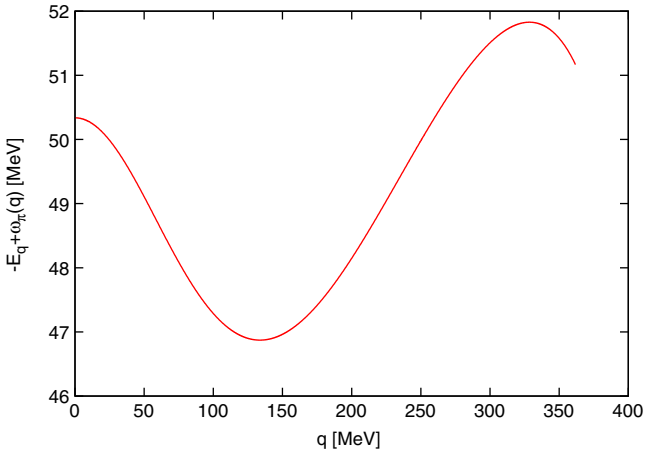

FIG. 6 (color online). Momentum dependence of $\mathcal{E}_{-}(q) = -E_q + \omega_\pi(q)$ at $T = 206$ MeV.

In the lower panel of Fig. 4, one finds that $\mathrm{Im}\Sigma^{+}(p_0)$ is divergent at four energies, $p_0 = \pm p_0^{(1)}$ and $\pm p_0^{(2)}$ with $p_0^{(1)} \simeq 47$ MeV and $p_0^{(2)} \simeq 52$ MeV. As shown in the small windows in the panel, $|\mathrm{Im}\Sigma^{+}(p_0)|$ is large in the range $p_0^{(1)} < |p_0| < p_0^{(2)}$. Through the Kramers-Kronig relation Eq. (18), this structure in $\mathrm{Im}\Sigma^{+}(p_0)$ in turn brings about the singularities in $\mathrm{Re}\Sigma^{+}(p_0)$ at $p_0 = \pm p_0^{(1)}$ and $\pm p_0^{(2)}$. These divergences are thus responsible for the emergence of the quasipoles discussed above, and hence the sharp peak at $p_0 \simeq 25$ MeV in $\rho_{+}(p_0)$.

To clarify the origin of the divergences in $\mathrm{Im}\Sigma^{+}(p_0)$, we show each part of $\mathrm{Im}\Sigma^{+}(p_0)$ in the decomposition of Eq. (23) in Fig. 5. The figure shows that the divergences come from $\mathrm{Im}\Sigma^{+}_{\pi\text{-pole}}(p_0)$, i.e., scattering of quarks with the bound pionic modes. As is seen from Eq. (24), this term takes nonzero values for p_0 satisfying Eq. (25). For $s = +1$, $\mathcal{E}_{+}(q)$ is a monotonically increasing function of q with the minimum $\mathcal{E}_{+}(0) = m + \omega_\pi(0) \simeq 270$ MeV at $q = 0$. Equation (25) thus has one solution for $rp_0 > m + \omega_\pi(0)$ with $r = \pm 1$, which, however, is outside the range of p_0 shown in Fig. 5. With $s = -1$, on the other hand, $\mathcal{E}_{-}(q) = -E_q + \omega_\pi(q)$ is not monotonic as shown in Fig. 6, and the range of $\mathcal{E}_{-}(q)$ is limited to $p_0^{(1)} < p_0 < p_0^{(2)}$. Therefore, $\mathrm{Im}\Sigma^{+}_{\pi\text{-pole}}(p_0)$ takes nonzero values for $p_0^{(1)} < |p_0| < p_0^{(2)}$. Note that the line of $\mathcal{E}_{-}(q)$ in Fig. 6 terminates around $q = 360$ MeV, because $\omega_\pi(q)$ enters the continuum and the bound pole disappears at this momentum as shown in Fig. 3. At the extrema of $\mathcal{E}_{-}(q)$, the relative group velocity $d\mathcal{E}_{-}(q)/dq$ vanishes. This leads to the divergence of the joint density of states $q^2|d\mathcal{E}_{-}(q)/dq|^{-1}$ and the singularity of $\mathrm{Im}\Sigma^{+}_{\pi\text{-pole}}(p_0)$ at $|p_0| = p_0^{(1)}$ and $p_0^{(2)}$. The divergences in $\mathrm{Im}\Sigma^{+}_{\pi\text{-pole}}(p_0)$ thus come from van Hove singularity owing to the divergence of the joint density of states.

We remark that the van Hove singularity discussed here does not manifest itself if $\omega_\pi(q)$ takes the relativistic form Eq. (10), since $\mathcal{E}_{-}(q)$ is then a monotonic function of q and $d\mathcal{E}_{-}(q)/dq$ remains nonzero for $q \neq 0$ [17]. Therefore, the van Hove singularity does not appear in the models composed of a fermion and boson with the hyperbolic dispersion relation assumed in Refs. [16–18]. The composite nature and medium effects that lead to a non-hyperbolic form of $\omega_\pi(q)$ play a crucial role for realizing the van Hove singularity and the drastic modification of the quark spectrum as a result of the singularity.

For the σ contribution, we see that there are small peaks in $\mathrm{Im}\Sigma^{+}_{\sigma}(p_0)$ at $|p_0| \simeq 130$ MeV. They come from the scattering of quarks with the sigma mode in the timelike region. Because this mode is always in the continuum, it does not form a singular structure in $\mathrm{Im}\Sigma^{+}_{\sigma}(p_0)$ unlike the pionic mode. On the other hand, as discussed above, the dynamic chiral susceptibility that lies in the spacelike region in the sigma mode has the maximum at $T = 206$ MeV. This contribution to the quark spectrum is, however, so small that it does not lead to a peak in $\mathrm{Im}\Sigma^{+}_{\sigma}(p_0)$. This is due to the fact that the critical point at which the chiral susceptibility diverges is far from this temperature and (zero) density in this model; it is located at $T \simeq 47$ MeV and the quark chemical potential $\mu \simeq 329$ MeV. Therefore, at the vanishing quark chemical potential, the contribution of the soft mode associated with this critical point is negligible at any temperature. Effects of the soft mode on the quark spectrum near the critical point will be investigated in Ref. [27].

B. Discussion

Here we shall closely examine the origin of the sharp peak in the quark spectrum in the far-soft region in terms of the van Hove singularity.

We first compare the quark spectrum in Fig. 4 with the results in Refs. [16–18] where the fermion spectra are computed in Yukawa models composed of an elementary

fermion and boson with masses m_f and m_b. Since the present analysis deals with the constituent quarks with $m \simeq 120$ MeV coupled to the bound pions with the rest masses $\omega_\pi(0) \simeq 150$ MeV and a vanishing width, the resultant quark spectrum may well be compared to the one obtained for the elementary particle systems with $m_f = m$ and $m_b = \omega_\pi(0)$. In Ref. [16], it is found that the spectrum of a massless fermion coupled with a massive boson has a three-peak structure with a sharp peak at the origin for $T \simeq m_b$. For a massive fermion, the peak position shifts toward nonzero positive energy, and gradually ceases to exist [17]; the range of m_f where the clear peak structure is realized is limited for $m_f/m_b \lesssim 0.2$. Now since the present mass ratio $m/\omega_\pi(0) \simeq 0.8$ is significantly larger than this upper limit, the quark spectral function should never have the peak structure, if the boson were described as an elementary particle with the free dispersion relation. It is also notable that the clear peak in Fig. 4 appears at an unexpectedly low energy, $p_0 \ll m$.

As already noted in the previous sections, the crucial difference of the present analysis from the ones in Refs. [16–18] is the compositeness of the bosonic modes with a nonhyperbolic dispersion relation due to the medium effect. Owing to the modified dispersion relation the van Hove singularity emerges in $\mathrm{Im}\Sigma^+(p_0)$, which significantly modifies the quark spectrum. On the other hand, the collective excitation corresponding to the quasipole at $p_0 \simeq 150$ MeV no longer makes a sharp peak because of the large decay rate. Here, the composite nature of the para-sigma and parapion is again responsible for this behavior, since the large decay rates around $p_0 = 150$ MeV come from the contribution of continuum spectra in the σ and π channels as shown in Fig. 5.

While we have emphasized the effect of the van Hove singularity on $\rho_+(p_0)$, we notice that the divergence is not necessarily indispensable for the drastic modification of the quark spectrum. The important feature is the existence of sharp peaks in $\mathrm{Im}\Sigma^+(p_0)$, i.e., a concentration of the decay rate of quasiquarks to some narrow energy regions. Such a sharp peak in $\mathrm{Im}\Sigma^+(p_0)$ in turn makes a sharp rise and decrease in $\mathrm{Re}\Sigma^+(p_0)$ through the Kramers-Kronig relation Eq. (18), and thus leads to a distorted quark spectrum. In fact, we will see in the next subsection that a somewhat moderate but still strong modification of the quark spectrum is realized even above T_{ZB} where the van Hove *singularity* no longer exists because of the absence of the stable pionic modes. When we incorporate the higher-order corrections, the bound pionic modes and quarks acquire nonzero decay widths and the would-be van Hove singularity will turn into a smeared peak. Even in this case, the modification of the quark spectrum and the emergence of a peak in a far-soft region is expected if a sharp peak exists in $\mathrm{Im}\Sigma^+(p_0)$. The modification of the quark spectrum induced by the scattering with a boson having a distorted dispersion relation, therefore, is expected to take place irrespective of the details of the model and approximation used in the present analysis.

As mentioned in Sec. II, the detailed form of the pion dispersion relation $\omega_\pi(q)$ in our model is affected by the cutoff scheme, and so is the detailed properties such as the position and strength of the van Hove singularity in the quark self-energy, although the drastic change of the quark spectrum itself takes place in a generic way once the dispersion relations of the parapion and quarks take non-hyperbolic forms in the medium. In fact, we have checked that the van Hove singularity in the quark self-energy emerges at some temperature even if we employ different regularization schemes in our model; while our model predicts a steep dispersion relation as shown in Fig. 3, the singularity appears even with a shallow dispersion relation of the pionic mode.

For determining the position and the strength of the van Hove singularity quantitatively, a precise determination of the spectral properties of the pionic mode, including its dispersion relation and width, near T_{ZB} is necessary. For this purpose, simulations on the lattice should hopefully be helpful.

C. High temperatures

Next, let us see the quark spectrum near and significantly above the pion zero-binding temperature T_{ZB}. In Fig. 7, we show the quark spectrum $\rho_+(p_0)$ and the corresponding self-energy $\Sigma^+(p_0)$ for $T = 0.98T_{\mathrm{ZB}}$, $1.02T_{\mathrm{ZB}}$, and $1.5T_{\mathrm{ZB}}$. It is found from the left panel of Fig. 7 that the van Hove singularity is not seen in the quark self-energy, although the stable pionic modes still exist at $T = 0.98T_{\mathrm{ZB}}$. This is because the momentum range where the stable pionic modes exist becomes narrow as T increases and the relative group velocity does not have a chance to vanish in the range. We, however, see that there exist sharp but finite peaks in $\mathrm{Im}\Sigma^+(p_0)$ at $|p_0| \simeq 55$ MeV. These peaks are understood as the remnant of the van Hove singularity in $\mathrm{Im}\Sigma^+(p_0)$ in Fig. 4. As a result of these peaks in $\mathrm{Im}\Sigma^+(p_0)$, three quasipoles manifest themselves with the same mechanism discussed in the previous subsection, and a sharp peak is formed at low energy $p_0 \simeq 16$ MeV. The position of this peak with the strength $Z \simeq 0.17$ is much lower than the constituent quark mass $m \simeq 100$ MeV for this temperature.

For $T > T_{\mathrm{ZB}}$, the stable pionic modes no longer exist, and hence the quark self-energy is smooth as a function of p_0. At $T = 1.02T_{\mathrm{ZB}}$, which is slightly above T_{ZB}, there exist broad peaks in $\mathrm{Im}\Sigma^+(p_0)$ around $p_0 \simeq \pm 76$ MeV. These peaks come from the coupling of quarks with the pionic modes; whereas the pionic modes are no longer stable, there still exists a well developed collective mode slightly above T_{ZB}. As a consequence of these peaks in $\mathrm{Im}\Sigma^+(p_0)$, a sharp peak is formed in $\rho_+(p_0)$ at $p_0 \simeq 12$ MeV with $Z \simeq 0.18$. The position of this peak is still considerably lower than the constituent quark mass $m \simeq 79$ MeV. The strong modification of the quark spectrum thus sustains even slightly above T_{ZB}.

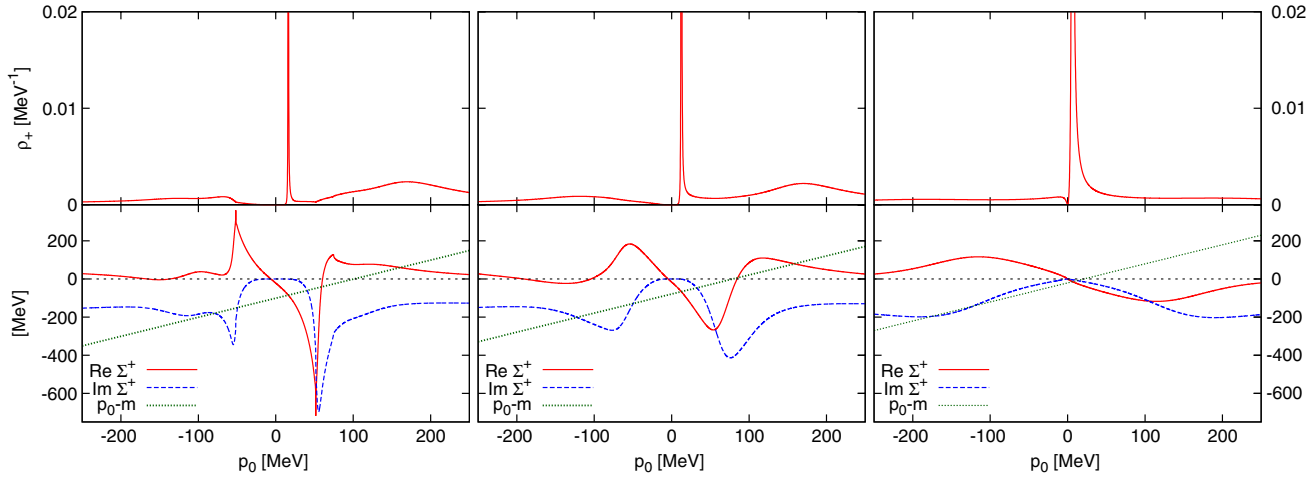

FIG. 7 (color online). Quark spectrum $\rho_+(p_0)$ and corresponding self-energy at $T = 0.98T_{\mathrm{ZB}}$ (left), $1.02T_{\mathrm{ZB}}$ (middle), and $1.5T_{\mathrm{ZB}}$ (right).

As T is raised further, the bump structure in $\mathrm{Im}\Sigma^+(p_0)$ disappears since the well-developed collective modes in the σ and π channels cease to exist. This behavior is seen in the right panel of Fig. 7, which presents the quark spectrum for $T = 1.5T_{\mathrm{ZB}}$. As a result, the quark spectrum approaches the mean field one as T increases. For $T = 1.5T_{\mathrm{ZB}}$, the position of the sharp peak of $\rho_+(p_0)$ is close to the the constituent quark mass $m \simeq 21$ MeV.

V. SUMMARY

In the present study, we have investigated the quark spectrum near the pseudocritical temperature T_{PC} of chiral phase transition and the pion zero-binding temperature T_{ZB} at vanishing quark chemical potential focusing on the effect of fluctuation modes in the σ and π channels in the two-flavor NJL model with nonzero current quark mass m_0. Compared with the previous study in the chiral limit [15], nonzero m_0 gives rise to the nonzero constituent quark mass m even above T_{PC} because of the crossover nature of the phase transition. In Ref. [17], it was shown in a Yukawa model where the boson has a dispersion relation valid in the free space that the nonzero fermion mass tends to suppress the appearance of the multipeak structures in the quark spectrum $\rho_+(p_0)$. Our microscopic model calculation has shown that $\rho_+(p_0)$ near T_{PC} is significantly modified by the scattering with stable pionic modes that have a nonhyperbolic dispersion relation, as was argued in various models in different contexts [21,22]. We have clarified that these modifications are caused by the van Hove singularity owing to the vanishing of the relative group velocity between quarks and bound pionic modes. The composite nature of the pionic modes that gives rise to the nonhyperbolic dispersion relation plays a crucial role for the modification of the quark spectrum. We have found that the quark spectrum has a sharp peak at an energy considerably lower than the constituent quark mass near T_{PC} as a consequence of the van Hove singularity.

Because our results show that the quark spectrum near T_{PC} is strongly modified by the scattering with pionic modes, it is interesting to pursue the effects of this modification on other observables near T_{PC}. For example, the existence of light quasiquark excitation would affect the T dependence of thermodynamic observables near T_{PC}. It would also affect the experimental observables in heavy ion collisions, such as the dilepton production rate [30]. Exploring the existence of the van Hove singularity in the early Universe in neutrino spectra and estimating their effects on the formation of baryon asymmetry [31] are also interesting subjects.

In this paper we have concentrated on the quark spectrum at zero momentum and evaluated the quark self-energy at the one-loop order. Since the medium near T_{PC} is thought to be a strongly correlated system, it is more desirable to adopt a more sophisticated approximation taking into account the self-consistency between the fluctuation modes and the quasiquarks, as was done for other problems in Ref. [9], in which the investigation is, however, not for the system close to T_{PC}, and the van Hove singularity is not seen. Indeed, as shown in the present work, when the system is far from T_{PC}, the peak in the quark spectrum is close to the one in the mean field approximation and the van Hove singularity does not occur. It would be quite interesting to investigate the quark spectrum near T_{PC} in such an approach. Such an investigation of the quark spectrum around the pseudocritical temperature is, however, beyond the scope of the present work and is left for a future project.

ACKNOWLEDGMENTS

This work is in part supported by JSPS KAKENHI Grants No. 25800148, No. 20540265, No. 23340067, No. 24340054, and No. 24540271. T. K. was partially supported by the Yukawa International Program for Quark-Hadron Sciences.

[1] I. Arsene *et al.*, Nucl. Phys. **A757**, 1 (2005); B. B. Back *et al.*, Nucl. Phys. **A757**, 28 (2005); J. Adams *et al.*, Nucl. Phys. **A757**, 102 (2005); K. Adcox *et al.*, Nucl. Phys. **A757**, 184 (2005).

[2] B. Muller, J. Schukraft, and B. Wyslouch, Annu. Rev. Nucl. Part. Sci. **62**, 361 (2012).

[3] Y. Aoki, G. Endrodi, Z. Fodor, S. D. Katz, and K. K. Szabo, Nature (London) **443**, 675 (2006); A. Bazavov *et al.*, Phys. Rev. D **85**, 054503 (2012).

[4] S. Borsanyi, Z. Fodor, S. D. Katz, S. Krieg, C. Ratti, and K. Szabó, J. High Energy Phys. 01 (2012) 138; A. Bazavov *et al.* (HotQCD Collaboration), Phys. Rev. D **86**, 034509 (2012); A. Bazavov *et al.*, Phys. Rev. Lett. **111**, 082301 (2013).

[5] F. Karsch and M. Kitazawa, Phys. Lett. B **658**, 45 (2007).

[6] F. Karsch and M. Kitazawa, Phys. Rev. D **80**, 056001 (2009).

[7] O. Kaczmarek, F. Karsch, M. Kitazawa, and W. Soldner, Phys. Rev. D **86**, 036006 (2012).

[8] M. Harada and Y. Nemoto, Phys. Rev. D **78**, 014004 (2008).

[9] D. Muller, M. Buballa, and J. Wambach, Phys. Rev. D **81**, 094022 (2010).

[10] J. A. Mueller, C. S. Fischer, and D. Nickel, Eur. Phys. J. C **70**, 1037 (2010).

[11] S.-X. Qin, L. Chang, Y.-X. Liu, and C. D. Roberts, Phys. Rev. D **84**, 014017 (2011); F. Gao, S.-X. Qin, Y.-X. Liu, C. D. Roberts, and S. M. Schmidt, arXiv:1401.2406.

[12] H. Nakkagawa, H. Yokota, and K. Yoshida, Phys. Rev. D **85**, 031902 (2012).

[13] M. Asakawa and T. Hatsuda, Phys. Rev. Lett. **92**, 012001 (2004); S. Datta, F. Karsch, P. Petreczky, and I. Wetzorke, Phys. Rev. D **69**, 094507 (2004); T. Umeda, K. Nomura, and H. Matsufuru, Eur. Phys. J. C **39**, 9 (2005).

[14] T. Hatsuda and T. Kunihiro, Phys. Lett. **145B**, 7 (1984); Phys. Rev. Lett. **55**, 158 (1985).

[15] M. Kitazawa, T. Kunihiro, and Y. Nemoto, Phys. Lett. B **633**, 269 (2006).

[16] M. Kitazawa, T. Kunihiro, and Y. Nemoto, Prog. Theor. Phys. **117**, 103 (2007); See also D. Satow, Y. Hidaka, and T. Kunihiro, Phys. Rev. D **83**, 045017 (2011).

[17] M. Kitazawa, T. Kunihiro, K. Mitsutani, and Y. Nemoto, Phys. Rev. D **77**, 045034 (2008).

[18] G. Baym, J. P. Blaizot, and B. Svetitsky, Phys. Rev. D **46**, 4043 (1992); Y. Hidaka, D. Satow, and T. Kunihiro, Nucl. Phys. **A876**, 93 (2012).

[19] M. Harada, Y. Nemoto, and S. Yoshimoto, Prog. Theor. Phys. **119**, 117 (2008).

[20] T. Hatsuda and T. Kunihiro, Phys. Rep. **247**, 221 (1994).

[21] A. B. Migdal, Rev. Mod. Phys. **50**, 107 (1978); T. E. O. Ericson and F. Myhrer, Phys. Lett. **74B**, 163 (1978); I. M. Mishustin, F. Myhrer, and P. J. Siemens, Phys. Lett. **95B**, 361 (1980); K. Kolehmainen and G. Baym, Nucl. Phys. **A382**, 528 (1982); C. Gale and J. Kapusta, Phys. Rev. C **35**, 2107 (1987); L. H. Xia, C. M. Ko, L. Xiong, and J. Q. Wu, Nucl. Phys. **A485**, 721 (1988); G. F. Bertsch, G. E. Brown, V. Koch, and B.-A. Li, Nucl. Phys. **A490**, 745 (1988); E. V. Shuryak, Phys. Rev. D **42**, 1764 (1990); CERN Report No. Cern-Th-5386/89, 1989 (unpublished).

[22] R. D. Pisarski and M. Tytgat, Phys. Rev. D **54**, R2989 (1996).

[23] L. Van Hove, Phys. Rev. **89**, 1189 (1953).

[24] G. E. Brown, E. Oset, M. V. Vacas, and W. Weise, Nucl. Phys. **A505**, 823 (1989).

[25] For a recent study on van Hove singularity in condensed matter physics, see, for example, G. Li, A. Luican, J. M. B. Lopes dos Santos, A. H. Castro Neto, A. Reina, J. Kong, and E. Y. Andrei, Nat. Phys. **6**, 109 (2009), and references therein.

[26] Y. Nambu and G. Jona-Lasinio, Phys. Rev. **122**, 345 (1961); **124**,246 (1961).

[27] M. Kitazawa, T. Kunihiro, and Y. Nemoto (unpublished).

[28] H. Fujii, Phys. Rev. D **67**, 094018 (2003); H. Fujii and M. Ohtani, Phys. Rev. D **70**, 014016 (2004).

[29] M. Kitazawa, T. Koide, T. Kunihiro, and Y. Nemoto, Prog. Theor. Phys. **114**, 117 (2005).

[30] E. Braaten, R. D. Pisarski, and T. C. Yuan, Phys. Rev. Lett. **64**, 2242 (1990); M. G. Mustafa, A. Schafer, and M. H. Thoma, Phys. Rev. C **61**, 024902 (1999).

[31] K. Miura, Y. Hidaka, D. Satow, and T. Kunihiro, Phys. Rev. D **88**, 065024 (2013).